

# The Physical Basis of Moisture Transport in a Cured Epoxy Resin System

V. B. GUPTA\* and L. T. DRZAL, *Materials Laboratory (AFWAL/MLBM), Wright-Patterson Air Force Base, Ohio 45433*, and M. J. RICH, *University of Dayton Research Institute, Dayton, Ohio 45469*

## Synopsis

The moisture transport characteristics of a difunctional epoxy resin cured with different amounts of metaphenylene diamine, using two cure cycles, are reported. Besides studying the kinetics of moisture sorption at 20, 50, 75, and 100°C, the investigations also included measurement of thermal expansion coefficients and dynamic mechanical transition of the dry and wet samples. The moisture sorption of the sample is shown to be related to its specific volume and hence to its fractional free volume. In the glassy state, the free volume is apparently in the form of frozen voids, and moisture sorption/desorption at this temperature is of the Langmuir type with little or no bond formation. At higher temperatures the free volume is generated predominantly through segmental motion of the  $\alpha$  transition. The Henry's Law mode becomes operative, and the moisture can now form bonds. The possible effect of non-uniform crosslink density on moisture sorption is also considered.

## INTRODUCTION

The transport of moisture in cured epoxy resin systems is an area of great practical importance in view of the effect of moisture on the properties of the cured resin and of the fiber-resin interphase in structural composites. Various studies of the kinetics of the moisture transport process,<sup>1-6</sup> the effect of moisture on the dynamic mechanical properties,<sup>7-9</sup> and the possible effect of heterogeneous morphology<sup>2,3,10-12</sup> have been reported. The non-Fickian nature of the sorption process has been noted<sup>1,4</sup> and attributed to damage resulting from the formation of cavities during the moisture exposure. The physical aspects of the transport process are receiving increasing attention, and the effects of free volume<sup>5</sup> and free volume distribution<sup>2</sup> are being recognized. Adamson has postulated<sup>2</sup> that the transport of moisture below  $T_g$  is a three-stage process in which the absorbed moisture first occupies the free volume present in the form of voids. In the second stage, water becomes bound to network sites causing swelling. Finally, in the third stage, water enters the densely crosslinked regions. The role of heterogeneous morphology has been inferred when (i) changes in free volume have apparently not been able to explain the results,<sup>3,11</sup> (ii) free volume was not considered as a possible parameter,<sup>10,12</sup> and (iii) new peaks or shoulders appeared in the dynamic transitions.<sup>13</sup>

In this investigation, a commercial epoxy resin based on diglycidyl ether of bisphenol-A (Epon 828, Shell) was cured with different amounts of an aromatic amine, metaphenylene diamine (mPDA), and its morphology, me-

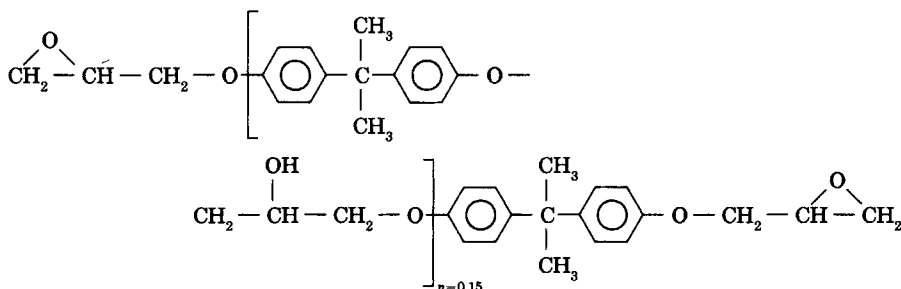
\*On leave from the Indian Institute of Technology, New Delhi 110016, India.

chanical properties, and moisture absorption characteristics studied. This paper describes the moisture absorption characteristics and then attempts to identify the roles played by crosslink density, free volume, and heterogeneous morphology in determining moisture absorption of this heterogeneous resin system.

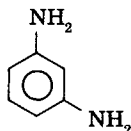
## EXPERIMENTAL

### Sample Preparation

The epoxy resin used was Epon 828 (Shell), which is based on diglycidyl ether of bisphenol-A (DGEBA) and has the following chemical structure:



The curing agent used was metaphenylenediamine having the following chemical structure:



The curing agent concentration for the stoichiometric composition, i.e., one in which the epoxy:amine ratio is 1:1, comes out to be 14.5 parts by weight per hundred parts of the resin (phr) for this system. In the present investigation samples were prepared containing 7.5, 10, 14.5, 20, and 25 phr of mPDA using the following procedure. The resin and the curing agent were heated in separate containers in an oven set at 75°C till the mPDA melted. They were then mixed by stirring, and the stirred mixture was vacuum-degassed for 7 min before being poured into flexible silicone rubber molds to form tensile dogbone coupons and rectangular rheometric bars. The curing cycle used was 75°C for 2 h followed by 125°C for 2 h. These samples will be designated as "standard cure." Another set of samples was prepared by postcuring the standard-cure samples at 175°C for 6 h in an inert gas environment; these will be referred to as the "post-cured" samples.

### Infrared Studies

Infrared studies were made in the near IR region on 1 mm thick discs and in the intermediate IR region on thin films cast between two caesium iodide windows.

### Specific Volume

The density at room temperature was determined in a sodium bromide-distilled water density gradient column. The coefficient of linear thermal expansion,  $\alpha$ , was measured on flat discs of about 1 mm thickness and 3 mm diameter from room temperature to above glass transition temperature at a heating rate of 10°C/min on a thermomechanical analyzer (TMA) interfaced to a computer. Since  $\alpha$  is very small and assuming that the sample is isotropic, the density at temperature  $T$ ,  $\rho_T$ , is given by

$$\rho_T = \rho_{T_r} / [1 + 3\alpha(T - T_r)]$$

where  $\rho_{T_r}$  is the density at room temperature ( $T_r$ ). The specific volume at temperature  $T$ ,  $1/\rho_T$ , was thus obtained. The measurement of thermal expansion coefficient by the TMA requires great care.<sup>14</sup> A number of measurements were made to ensure consistency of results.

### Dynamic Mechanical Transitions

The dynamic mechanical spectra were recorded on a DuPont Dynamic Mechanical Analyzer 1090 (DMA) and on a Rheometrics Mechanical Spectrometer (RMS). From the rubbery modulus (modulus above  $T_g$ ) obtained in torsion ( $G'$ ), the molecular weight between crosslinks,  $M_c$ , was calculated using the following approximate expression<sup>15</sup>:

$$\log_{10} G' = 7 + \frac{293\rho}{M_c}$$

where  $\rho$  is the density. For a highly crosslinked system like cured epoxy resin, this expression has been shown<sup>15,16</sup> to lead to better agreement between theory and experiment.

### Moisture Sorption and Desorption Studies

For moisture sorption studies, thin plates approximately 15 × 11 × 1 mm, sliced from the end tabs of tensile coupons, were used. The samples were exposed to a 100% relative humidity environment at 20, 50, 75, and 100°C. The moisture absorbed by the sample was determined gravimetrically. The percent moisture absorbed at time  $t$ ,  $M_t$ , was plotted as a function of  $\sqrt{\text{time}/b}$ , where  $b$  is the sample thickness. Extrapolation of these kinetic curves to infinite time gives the equilibrium moisture uptake  $M_\infty$ . The apparent diffusion coefficient  $D$  can then be calculated from the following expression:

$$\frac{M_t}{M_\infty} = \frac{4}{b} \frac{Dt^{1/2}}{\pi}$$

Limited studies on desorption were made by leaving the sample at the corresponding sorption temperature in a dry environment for fixed times and then monitoring the moisture content gravimetrically.

## RESULTS AND DISCUSSION

## General Characterization

The glass transition temperatures of the various samples, as obtained from the peak positions of  $\tan \delta$  on the RMS at a frequency of 0.016 Hz, are shown in Figure 1. The values of molecular weight between crosslinks,  $M_c$ , calculated from the rubbery torsional modulus, are shown in Figure 2. As expected, the stoichiometric sample has low  $M_c$  or high crosslink density and a high  $T_g$ ; on either side of stoichiometry, both crosslink density and  $T_g$  decrease. Post-curing results in a considerable increase in the crosslink density and the  $T_g$  of the epoxy-rich samples, but the effect on the other samples is very slight.

## Infrared Results

Infrared studies showed that the 7.5 and 10 phr "standard-cure" samples contained a considerable amount of unreacted epoxy groups while the 20 and 25 phr samples had unreacted amines. The stoichiometric sample (14.5 phr) also contained small amounts of unreacted epoxy and amine groups. On post-curing, the 10 phr sample showed the most dramatic reduction of unreacted epoxy groups followed by the 7.5 phr samples. The stoichiometric sample now had no detectable unreacted groups. Some further curing also occurred in the 20 and 25 phr samples. In the epoxy-rich samples, further crosslinking had apparently occurred by reaction between the epoxy and the hydroxyl groups. Since 175°C is close to the maximum curing temperature ( $T_{c\infty}$ ) of the stoichiometric sample,<sup>17</sup> the post-curing apparently results in more fully cured samples whose chemistry would be expected to remain essentially unchanged during the moisture sorption cycle and also during the thermal and mechanical measurements. The bulk of the discussion will therefore be on these samples.

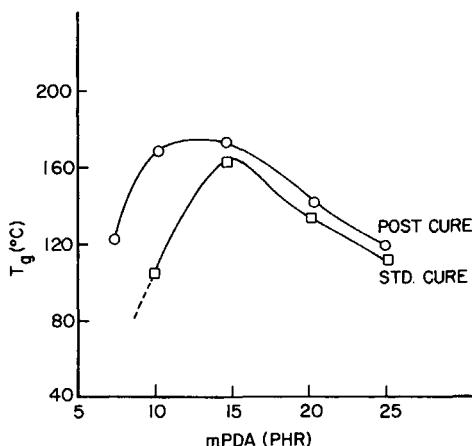


Fig. 1. The dependence of glass transition temperature on curing agent concentration.

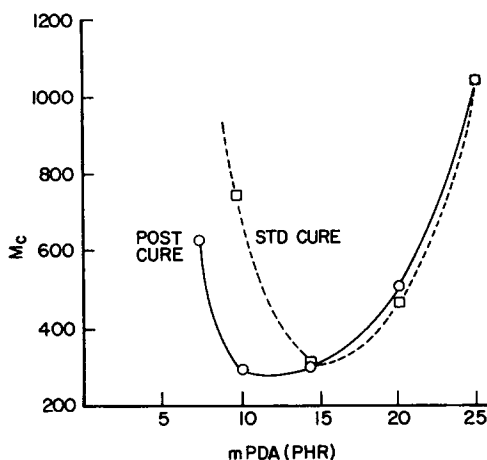


Fig. 2. The dependence of molecular weight between crosslinks ( $M_c$ ) on curing agent concentration.

### Specific Volume and Free Volume

The temperature dependence of specific volume was computed by combining the room temperature density data with the thermal expansion data. Since thermal expansion depends on the variations in the interatomic forces with temperature for a solid<sup>18</sup> and for the most part reflects the increase in fractional free volume in the case of liquids,<sup>19</sup> this procedure is justified as an approximate measure of specific volume. Since occupied volumes for the various samples are not known, free volume cannot be directly computed. However, in keeping with the general practice in the literature,<sup>3,5</sup> the present discussion will be limited to specific volume which itself will be treated as a measure of free volume. The shortcomings of this approach<sup>20-23</sup> should, however, be kept in mind.

The room temperature density data are shown in Figure 3. It is seen that the sample having the highest crosslink density and  $T_g$  in the standard-cure series (14.5 phr) has the lowest density. On post-curing, density decreases; it has already been shown (Fig. 1) that post-curing increases  $T_g$ . The line marked as "baseline" in Figure 3 represents the calculated density of a physical mixture of Epon 828 and mPDA which have densities of 1.168 g/cc and 1.135 g/cc, respectively.<sup>24</sup> For this calculation the rule of mixtures was used and additivity of specific volumes assumed. It is observed that as the curing agent concentration increases, the calculated density of the mixture falls. The measured density curve for the cured sample, however, shows that the density of the amine-rich samples actually increases with increasing mPDA concentration. This is indicative of the relatively closer packing in these samples. If the baseline is taken as the reference line for a qualitative estimate of free volume, some anomalies reported in the literature<sup>3,11</sup> may actually need reconsideration.

The thermal expansion data for the post-cured samples are shown in Figure 4. In the glassy state, the thermal expansion coefficients ( $\alpha_g$ ) for the

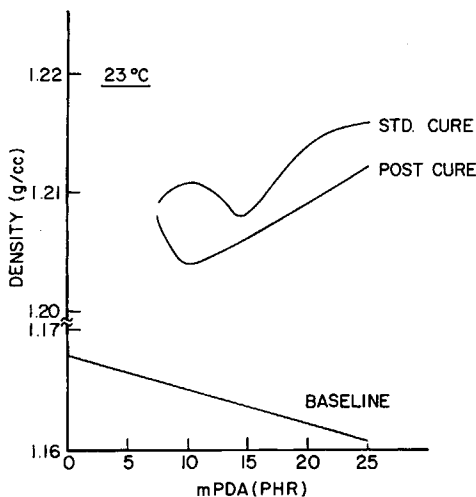


Fig. 3. The variation of room temperature density with curing agent concentration (baseline explained in the text).

various samples are not very different; the slightly lower values for the amine-rich samples may be taken as a reflection of their better packing. In the rubberlike state, the most highly crosslinked sample has the lowest thermal expansion coefficient ( $\alpha_L$ ), indicating that the network is tight, as expected.<sup>25</sup>

The specific volumes calculated from the room temperature density and the thermal expansion data are shown in Figure 5. It is noteworthy that the specific volumes of samples of different stoichiometry undergo a reversal with temperature. Samples having high  $T_g$ 's (10 and 14.5 phr) have the highest specific volumes at room temperature and the lowest at the higher temperatures. Samples having low  $T_g$ 's (7.5 and 25 phr) have the lowest specific volumes at room temperature and the highest at the higher temperatures. The possible reasons for this have been discussed in detail elsewhere.<sup>26</sup>

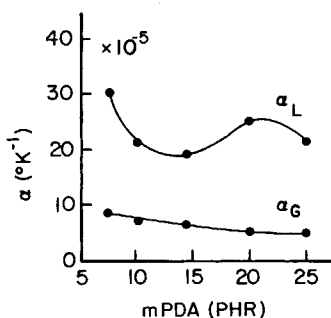


Fig. 4. The variation of the coefficient of linear thermal expansion of the post-cured samples below ( $\alpha_G$ ) and above ( $\alpha_L$ )  $T_g$  with curing agent concentration.

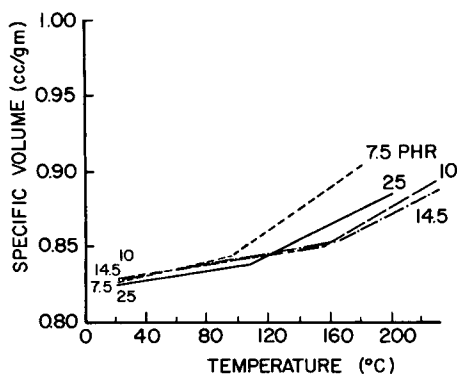


Fig. 5. The dependence of specific volume on temperature for the post-cured samples.

### Some General Effects Due to Moisture

Some general effects due to the presence of moisture in these samples will first be presented. The thermal expansion characteristics of the wet, post-cured samples containing moisture close to the equilibrium levels (3–6% moisture introduced at 90°C) are presented in Figure 6. A comparison with Figure 4 shows that the presence of moisture results in a considerable increase of the expansion coefficient above  $T_g$ . The highly crosslinked sample has still the lowest expansion coefficient. It has been shown<sup>27</sup> that the thermal expansion coefficient of Fiberite 934, another cured epoxy resin system, is a function of the amount of moisture. In the present case, the moisture content of the samples was close to their equilibrium values, and thus the  $T_g$ 's show considerable reduction, as shown in Figure 7. The specific

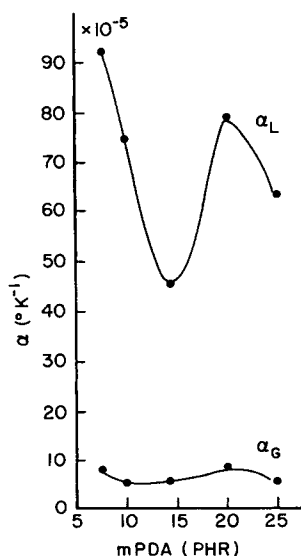


Fig. 6. The coefficient of linear thermal expansion of the wet post-cured samples below ( $\alpha_G$ ) and above ( $\alpha_L$ )  $T_g$ .

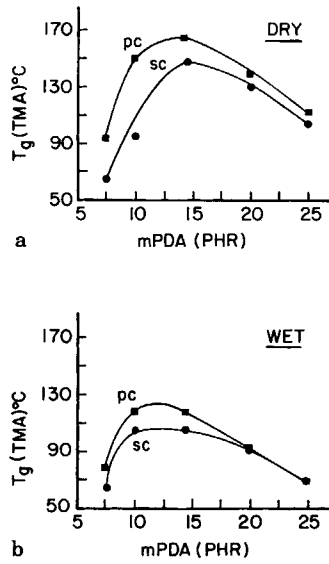


Fig. 7. The glass transition temperatures of the various samples as obtained from the TMA: (a) dry; (b) wet.

volumes of the wet samples were calculated from the room temperature density data presented earlier (Fig. 3) and the expansion coefficient data (Fig. 6). As shown in Figure 8, the specific volume changes are now much greater than those for the dry samples (Fig. 5).

### Dynamic Mechanical Transitions

The dynamic mechanical studies were made on post-cured rectangular rheobars both in the dry and wet states; in the latter case moisture was introduced at temperatures between 50 and 100°C for varying times so that the samples had absorbed moisture close to 2–3.5%. The main interest in making these studies was to understand how the relaxation processes in the polymer interrelate with moisture sorption. The  $\alpha$ -relaxation was stud-

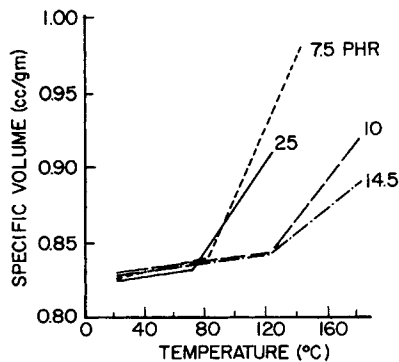


Fig. 8. The specific volume of the wet post-cured samples.



ied with the help of DuPont's Dynamic Mechanical Analyzer (DMA). The sensitivity of this instrument was not sufficient to resolve the  $\alpha'$ -relaxation, which is a weak relaxation between the  $\beta$ - and  $\alpha$ -relaxations, and has been discussed in detailed elsewhere.<sup>26</sup> Therefore, the rheometrics mechanical spectrometer (RMS), which has a relatively higher sensitivity, was used to study the  $\alpha'$ -relaxation.

### The $\alpha$ -Relaxation

The  $\tan \delta$  curves were recorded on a DMA as the sample was being heated at a rate of 10°C/min, and the data for the various samples are shown in Figure 9. The  $\alpha$  peak in most cases appears to be split into a doublet separated by about 40°C. The  $\tan \delta$  curves were also recorded during the cooling of the sample at 10°C/min after the sample had been rapidly heated to above its  $T_g$ . The results were broadly similar in the two cases. The splitting of the peak into a doublet was observed in a separate preliminary study reported earlier,<sup>28</sup> where it was postulated to result either from non-uniform drying of the sample or from their heterogeneous, two-phase morphology. Electron microscopic evidence has been presented<sup>29</sup> for the existence of heterogeneities within these samples which are microscopic regions of relatively higher crosslink density. To gain further understanding of this problem, the dynamic experiments were conducted in a closed, moist environment to minimize the drying of the sample. The rectangular rheobars were encapsulated in thin (0.002 in. thick), sealed stainless steel sacs by The Sentry Company, Foxboro, MA. The  $\tan \delta$  data for some post-cured, wet encapsulated samples was then obtained by first heating the sample very fast to above its  $T_g$  and then recording the spectra during cooling at the rate of 10°C/min. This was done for two reasons. First, it was expected that less moisture would leave the sample during the experiment, and, secondly, the transient effects due to aging would not be observed. As shown in Figure 10, the doublet does not appear now; the  $\alpha$ -relaxation, however, shifts to lower temperatures. For the stoichiometric sample (14.5 phr), the

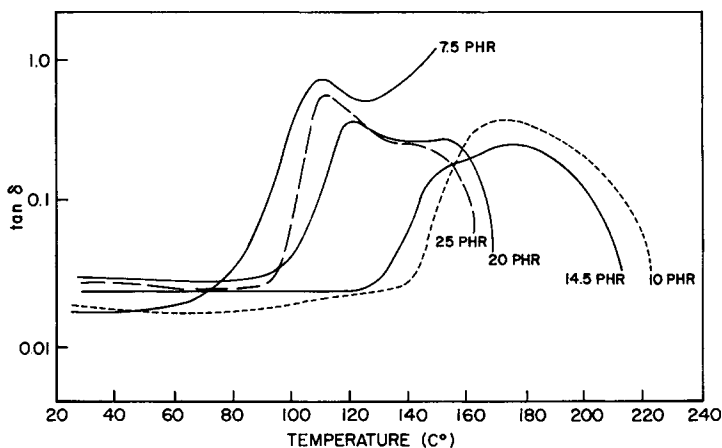


Fig. 9. The DMA dynamic transition ( $\tan \delta$ ) data for the wet post-cured samples.

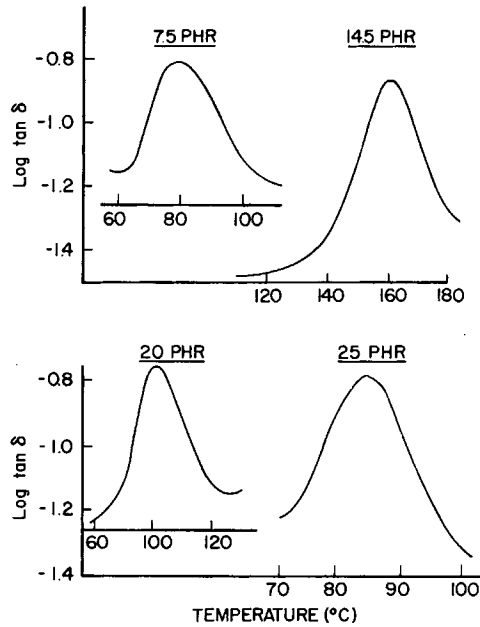


Fig. 10. The DMA dynamic transition ( $\tan \delta$ ) data for the encapsulated wet post-cured samples.

data on the dry encapsulated sample, wet encapsulated sample, and wet sample without encapsulation are shown together in Figure 11. The lower  $\tan \delta$  values for the encapsulated specimens arise presumably due to the contribution of the steel encapsulation which will affect the storage modulus  $E'$  and the loss modulus  $E''$  and therefore  $\tan \delta$  which is  $E''/E'$ . The presence of a single peak in the wet specimen suggests that the previously observed doublets were probably due to the nonuniform drying of the specimen during the experiment. However, the amplitudes of the  $\alpha$ -relaxation in the dry and

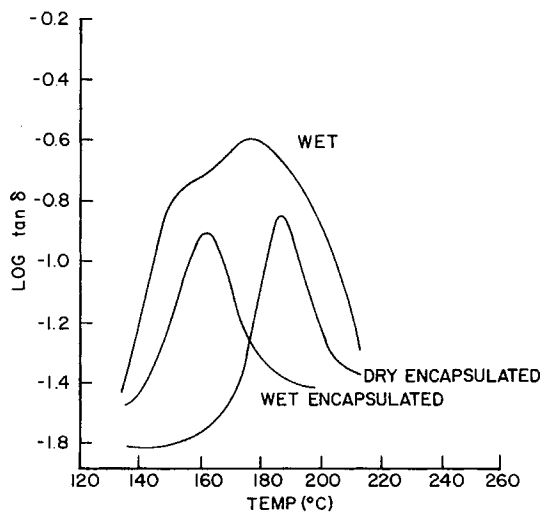


Fig. 11. The DMA dynamic transition ( $\tan \delta$ ) data for the post-cured stoichiometric samples.

wet-encapsulated samples are seen to be quite close in value. The amplitude of  $\tan \delta$  is a measure of the intensity of the relaxation, and this did not appear to be affected much by moisture. However, as the sample cooled to below  $T_g$ , the wet sample showed higher loss.

### The $\alpha'$ -Relaxation

The  $\alpha'$ -relaxation appears close to room temperature in the wet samples and therefore can play an important role in determining the moisture absorption characteristics of the sample in this temperature range. This relaxation, as stated elsewhere,<sup>26</sup> could arise either from nonequilibrium stresses frozen-in during the cooling part of the cure cycle or from relaxation in the less densely crosslinked phase in the sample. In either case it would be expected to be moisture-sensitive. The  $\tan \delta$  curves were recorded during cooling of the sample on the RMS. Only the results for the two samples with low  $T_g$  (7.5 and 25 phr) are presented in Figures 12(a) and (b), respectively, since they show up the effects of moisture more clearly because of less drying during the experiment. The  $\alpha$ -relaxation part of the loss spectra are also included in the figures wherein doublets are observed as in the case of the DMA studies. The wet  $T_g$ 's as obtained from the peak positions of  $\tan \delta$ , are only slightly higher than the wet  $T_g$ 's obtained from the TMA (Fig. 7), presumably due to the higher frequency of the RMS. The weak  $\alpha'$  peaks are seen to be close to room temperature and are reasonably well resolved. Their amplitudes are higher in the wet samples. A similar moisture-sensitive peak has been reported for another cured epoxy resin system,<sup>9</sup> where it has been designated as the  $\omega$  peak.

### Sorption Kinetics

The moisture absorption data for the postcured samples is presented in Figure 13 as percent absorbed water vs.  $\sqrt{\text{time}/b}$ , where  $b$  is the sample thickness, for the 7.5, 10, 14.5, 20, and 25 phr samples. For some samples

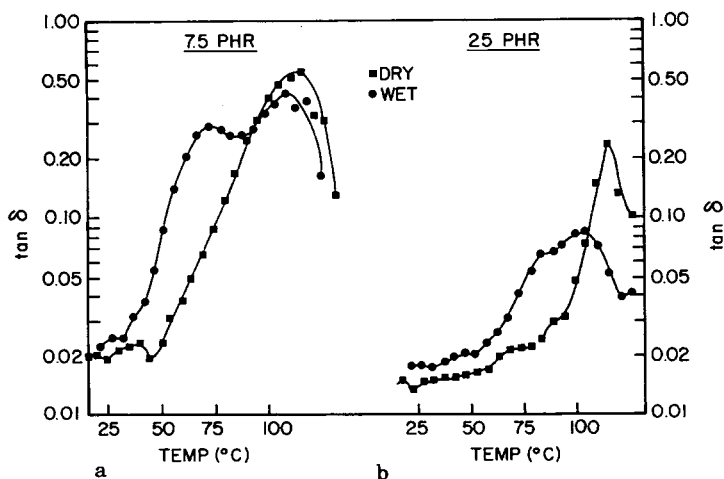


Fig. 12. The RMS dynamic transition ( $\tan \delta$ ) data for the dry and wet post-cured samples with (a) 7.5 and (b) 25 phr of curing agent.

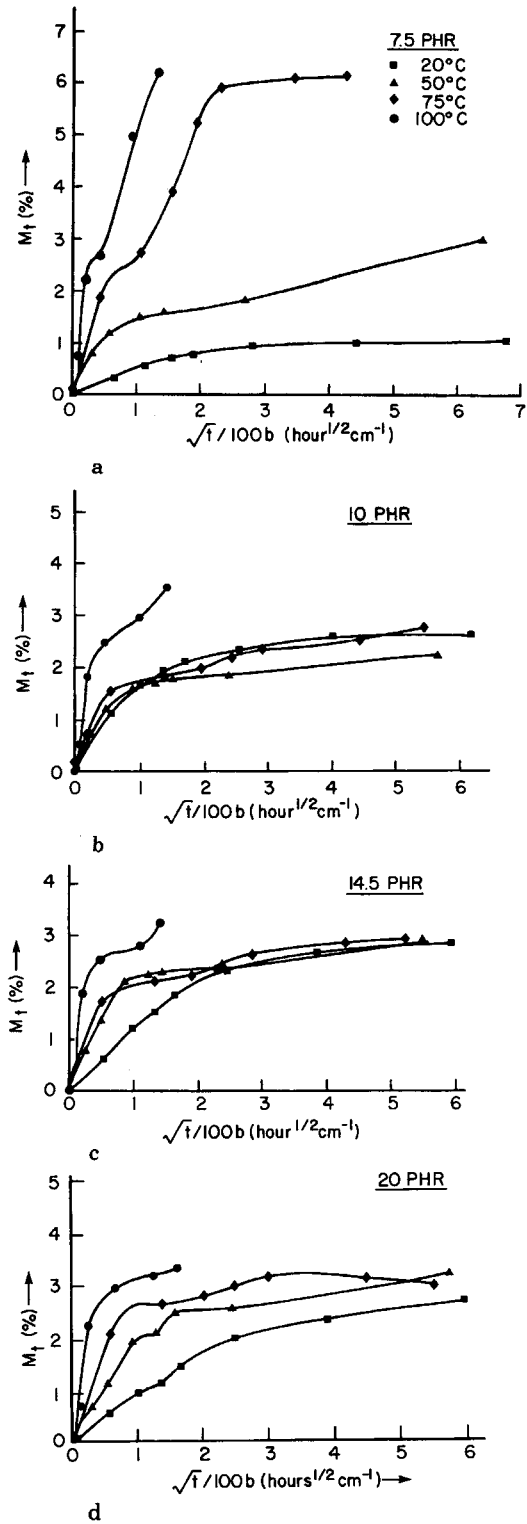


Fig. 13. Moisture sorption data for (a) 7.5, (b) 10, (c) 14.5, (d) 20, and (e) 25 phr post-cured samples: (■) 20°C; (▲) 50°C; (◆) 75°C; (●) 100°C.

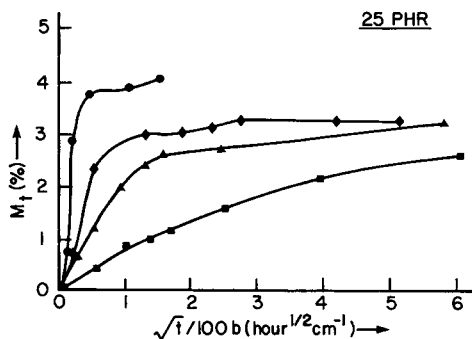


Fig. 13. (continued from previous page)

moisture sorption appears to proceed in two stages. However, broadly speaking, the sorption process shows the usual features: viz., (a) the initial diffusion-controlled linear region which shows considerable temperature dependence. Interestingly, the temperature dependence of the initial region is relatively small for the most highly crosslinked, high  $T_g$  samples (14.5 phr and 10 phr) and is high for the less crosslinked, low  $T_g$  samples. (b) At longer times, the moisture uptake appears to be rather less dependent on temperature. The temperature dependence in this region is also relatively large for samples of low crosslink density/low  $T_g$ .

The results presented in Figures 14(a) and (b) show that at room temperature, the most highly crosslinked samples absorb the maximum moisture, while at 100°C they absorb the least. It is noteworthy that there is a reversal both in the rate of absorption and the final amount absorbed between these two temperatures. It may be recalled that such a reversal had earlier been observed in the case of the wet specific volumes also. The data on wet specific volume, the diffusion coefficient, and the equilibrium mois-

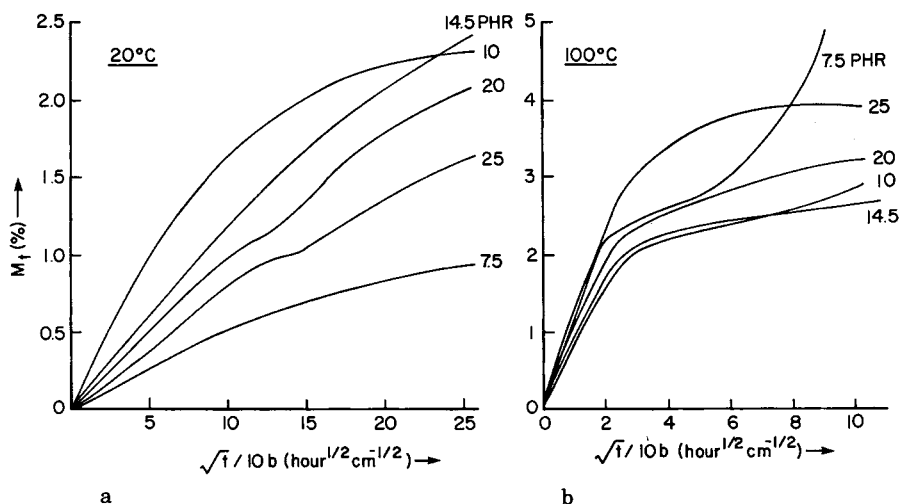


Fig. 14. Moisture sorption data at (a) 20°C and (b) 100°C for post-cured samples of different stoichiometries.

ture uptake at 20 and 100°C are shown in Figures 15(a), (b), and (c), respectively. It is obvious that the specific volume and hence the free volume plays an important role in determining the moisture absorption characteristics of the post-cured samples. Small differences in specific volume between the samples at room temperature are seen to result in considerable differences in their diffusion coefficients. At 100°C, on the other hand, large differences in specific volume lead to only small differences in diffusion coefficient.

In calculating the diffusion coefficient, a major difficulty arises in the selection of a suitable value for the equilibrium moisture uptake, particularly for samples which show a two-stage sorption process. The values of  $M_{\infty}$  for calculating the diffusion coefficient shown in Figure 15(b) were obtained by extrapolating the first stage sorption curves. This was done because the diffusion process should reflect the mechanism of initial sorption. There is a considerable approximation involved in such an arbitrary extrapolation. It was therefore decided to use another parameter to characterize this process which would not require the arbitrary extrapolation procedure. This parameter was taken as the slope of the initial linear portion of the kinetic curves presented in Figures 15 and will be called the "initial sorption rate."

### The Initial Sorption Rate

The initial sorption rate is plotted as a function of wet specific volume in Figure 16. As expected, the initial sorption rate is low at room temperature and high at high temperature. However, at room temperature small changes in free volume affect the initial sorption rate by a considerable amount, resulting in an increase by a factor of 4–5 while at the higher temperature (100°C), large changes in free volume have only a very small effect on the initial sorption rate, viz., the increase is less than a factor of 2 at this temperature. This is similar to the effect on diffusion coefficient observed earlier. The dependence of mobility on free volume has been considered in detail by Struik.<sup>23</sup> The first important point made by Struik is that even when the specific volume is far from its equilibrium value, it uniquely determines the relaxation times and therefore the free volume

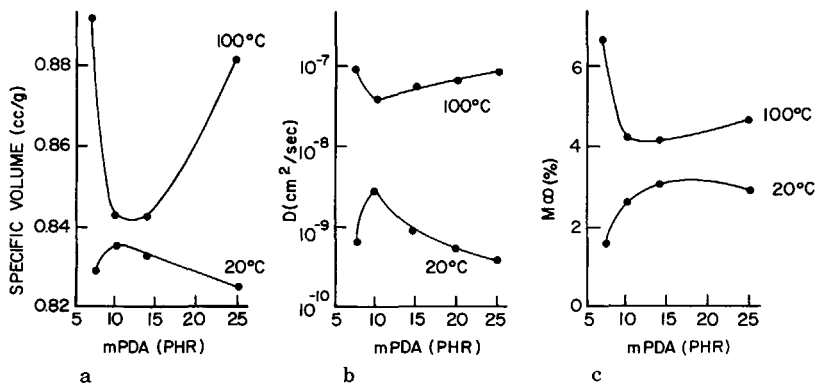


Fig. 15. The wet specific volume (a), the diffusion coefficient (b), and the equilibrium moisture uptake (c) at 20 and 100°C for the post-cured samples.

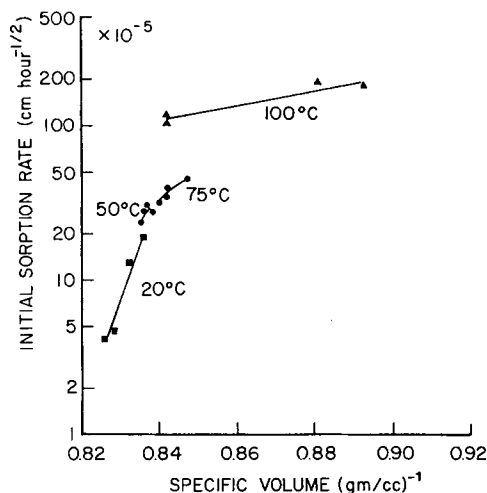


Fig. 16. The initial sorption rate at various temperatures as a function of wet specific volume for the post-cured samples.

concept is applicable even for nonequilibrium state. Then Struik invokes the concept introduced by Cohen and Turnbull<sup>30</sup> that only the few large holes of a size comparable to that of the molecules contribute to the mobility. Data is then presented to show that the change in mobility with free volume is larger in the nonequilibrium state below  $T_g$  than above  $T_g$ . This effect increases with decreasing temperature. Thus, at lower temperatures, though free volume is very small, the free volume distribution is such that the mobile (larger) holes still make a considerable contribution to mobility and large changes in mobility are still possible even though the changes in free volume are very small.

### The Two Modes of Sorption

Another factor that should be considered at this stage is that there are two modes of sorption in glassy polymers: the Langmurian mode involves the entry of water molecules into preexisting gaps while in the Henry's law mode; the water molecules enter through gaps created by segmental motion.<sup>31</sup> It has been pointed out by Michaels et al.<sup>32</sup> that since water molecules in the Langmurian mode sorb in the voids already present in the sample, little energy is needed. More energy is needed for a molecule to enter the Henry's law mode since separation of polymer chains is needed for dissolution by this mechanism. For the post-cured samples, the wet  $T_g$  is around 120°C for the highly crosslinked samples and 70–90°C for others. Since moisture sorption studies have been made between 20 and 100°C, the dual mode mechanism will be operative to varying extents in these samples. Below  $T_g$ , the initial diffusion involves the Langmuir mode, and, since little energy is needed for this transport process, small differences in free volume can make a considerable difference to the amount of moisture sorbed. At higher temperatures, the Henry's law mode will become relatively more important, and, since this involves more energy, the effects of the differences in free volume on diffusion will become relatively less pronounced.

### Temperature Dependence of Free Volume Below $T_g$

The present results on moisture sorption bring out another important point. The data on moisture sorption for the high  $T_g$  samples (10 and 14.5 phr), which have high free volume at room temperature, show (Figs. 13) that the room temperature moisture sorption at long times can be as large as or larger than the moisture sorption at 50°C or even at 75°C. This observation suggests that below  $T_g$  free volume can increase with decrease of temperature. This aspect will now be considered briefly.

It was postulated by Fox and Flory<sup>33</sup> and later by Williams, Landel, and Ferry<sup>34</sup> that the fractional free volume of polymers below  $T_g$  is constant. In the case of cured epoxy resin, Adamson has suggested<sup>2</sup> that below  $T_g$  free volume increases with decrease of temperature and this increase is essentially because of a reduction in the amplitude of Van der Waals motion. The consequent reduction in the occupied volume results in an increase of free volume. When this happens close to the equilibrium state, the bound water can become unbound, and thus, at lower temperature, more water can diffuse into the specimen. It has been shown by Patton et al.<sup>35</sup> that, for the sorption of benzene in poly(ethylene terephthalate) below  $T_g$  (83°C), Langmuir capacity increases by a factor of 2 as temperature decreases from 60 to 20°C.

### Measurement of the Langmuir Capacity

A measure of the Langmuir capacity can be obtained if the fraction of water going into the preexisting gaps can be determined. Recently studies on poly(methyl methacrylate) have been reported,<sup>36,37</sup> where the amount of water going into the voids has been calculated by making measurements at room temperature of the weights of the moisture-containing samples in air ( $W_{a,t}$ ) and in water ( $W_{w,t}$ ); the fraction of water in microvoids is given by

$$\frac{W_{w,t} - W_{w0}}{W_{a,t} - W_{a0}}$$

where  $W_{w,0}$  and  $W_{a,0}$  are the initial weights in water and air, respectively. This fraction may be taken as the microvoid fraction. For the post-cured stoichiometric sample, such measurements of weight were made at room temperature in air and in water on samples which had earlier been exposed to 100% relative humidity at 20, 50, 75, and 100°C for short times so that they had absorbed moisture up to about 1.5% at these temperatures. Two sets of measurements were made. Both gave consistent results and the average values are shown in Figure 17. When water is absorbed at room temperature, a large fraction of the absorbed moisture enters the voids; but when water sorption is at higher temperatures, the fraction of water going into the voids is considerably less. These results thus confirm that, at room temperature, the Langmuir mode will be predominant while at higher temperatures, the Henry's law mode can become increasingly more effective.



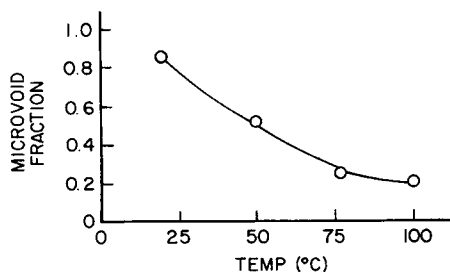


Fig. 17. The microvoid fraction in the post-cured stoichiometric sample at different temperatures.

In spite of the availability of higher free volume at lower temperatures, the initial diffusion rate in general increases with increasing temperature as is normal for a thermally activated process. As the free volume gets progressively filled up, the rate of sorption decreases. At longer times, for the high  $T_g$  samples (10 and 14.5 phr), there can be more moisture in the sample subjected to 20°C sorption than one subjected to 50°C or even 75°C sorption. This suggests that, during room temperature sorption, there can be more fractional free volume than at 50° or 75°C. The specific volume, however, increases with increasing temperature.

#### An Alternative Mechanism for the Increase in Free Volume

The mechanism responsible for the higher free volume at lower temperatures suggested by Adamson<sup>2</sup> would apply to all polymers in general and has been briefly described earlier. For a heterogeneous system composed of rigid inclusions in a soft matrix, a different mechanism was proposed<sup>38</sup> to explain the increase in free volume with decrease in temperature for a carbon-black-filled elastomer. Since this mechanism may be applicable to the cured epoxy resin system under consideration because of its heterogeneous nature,<sup>29</sup> it will be briefly described here. In a heterogeneous system, the coefficient of expansion of the matrix, both in the rubbery and glassy states, is greater than that of the rigid heterogeneity. Cooling the polymer results in stresses being set up around the rigid phase. Above  $T_g$ , the stresses can be relieved because flow can take place. Below  $T_g$ , the stresses will become large and will not be relieved rapidly. The matrix in the immediate vicinity of the rigid phase will be in biaxial tension, and, since the Poisson's ratio of glassy polymers is less than 0.5, there will be dilatation. The amount of dilatation will increase as the temperature is lowered further below  $T_g$ . Superimposed on the normal thermal contraction of the matrix, the effect of the dilatation will be a reduction of the coefficient of thermal expansion of the polymer and an apparent increase in free volume. In the cured epoxy resin, the heterogeneities, which are regions of high crosslink density, will form the rigid phase and the less crosslinked regions will form the matrix. It may be emphasized that while the previous mechanisms<sup>2,37</sup> invoked changes in occupied volume with temperature as being responsible for higher free volume at low temperature, this scheme

suggests that the temperature dependence of the total specific volume itself is reduced, and this can therefore result in the anomalous effect, viz., an increase of fractional free volume with decrease of temperature.

### Effect of Cure Cycle

It has already been shown that on post-curing the densities of all the standard-cure samples decrease (Fig. 3); the largest decrease being for the 10 phr sample. The decrease of density is accompanied by and in fact is a result of an increase in crosslink density and of  $T_g$ .<sup>26</sup> Since the chemistry of the standard-cure samples changes when taken to above their  $T_g$ 's, the thermal expansion coefficient data above  $T_g$  is not representative of the original material and will therefore not be reported. Below  $T_g$  the data are shown in Figure 18 and for comparison the data for the post-cured samples are also included; they are broadly similar. From the room temperature density and expansion coefficient, the specific volume at different temperatures was calculated. As shown in Figure 19, in all cases the post-cured samples have higher specific volumes up to 100°C.

The sorption kinetic curves for the standard-cure samples are shown in Figure 20. The principal features of these curves are similar to those of the postcured samples (Fig. 13), but they show relatively greater temperature dependence. The initial sorption rate and equilibrium moisture uptake,  $M_\infty$ , extracted from these kinetic curves are shown in Figures 21(a) and (b), respectively. For comparison the results for the post-cured samples are also included. The room temperature results show the maximum differences, as observed previously. The higher initial sorption rate and  $M_\infty$  of the post-cured samples at room temperature are due to their relatively higher free volume.

The free volume dependence is further confirmed when the data for the room-temperature-cured sample is examined along with the other data. For the stoichiometric sample (14.5 phr), the room-temperature sorption curves for the room-temperature-cured, standard-cure, and post-cured samples are shown in Figure 22 along with the density data. The sample with the highest crosslink density and the highest  $T_g$  has the lowest density and absorbs the highest amount of moisture. The sample with the lowest crosslink density has the highest density and absorbs minimum amount of moisture.

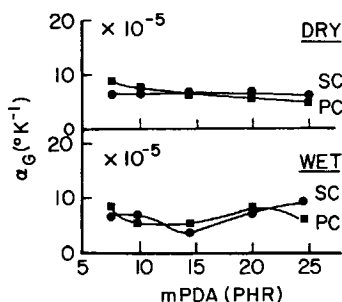


Fig. 18. The coefficient of thermal expansion below  $T_g$  ( $\alpha_G$ ) for the standard-cure and post-cured samples.

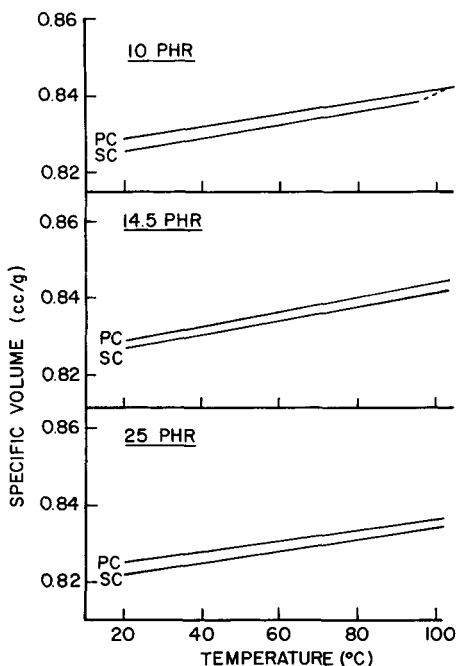


Fig. 19. Temperature dependence of specific volume of standard-cure and post-cured samples containing 10, 14.5, and 25 phr of curing agent.

### Dependence on Relaxation Processes

The data presented in Figures 9–12 showed that both the  $\alpha'$ - and  $\alpha$ -relaxations occur over a wide temperature range. The contributions of these relaxations to moisture transport at different temperatures will therefore be to varying extents. First the mechanical relaxation data for the standard-cure and post-cured samples will be compared with the aim to understand the dependence of moisture sorption on the relaxation processes. Since the wet samples dehydrate during the dynamic mechanical test, the following procedure was adopted to maintain consistency. The  $\tan \delta$  curves obtained on the RMS at a frequency of 0.016 Hz for the dry samples were shifted on the temperature axis so that the  $\tan \delta$  peak of the dry sample, whose values are given in Figure 1, coincided with the wet  $T_g$  as obtained on the TMA [Fig. 7(b)]. One of the limitations of this procedure is that it neglects the effect of water on the intensity of the  $\tan \delta$  relaxation. Nevertheless, as shown presently, it gives useful information, and the data are summarized in Figure 23. The following points are noteworthy:

(i) As temperature increases, the relaxation peaks become more intense and the areas of the peaks become much greater in the 7.5 and 25 phr samples. For the other two samples, the relaxation intensities remain relatively low and the areas smaller. As shown earlier in Figure 21(a), the initial sorption rate shows a considerable increase in the 20–100°C range for the 7.5 and 25 phr samples (by a factor of 25–60), while the increase is

small for the other two samples (by a factor of 5–15). The interdependence of free volume and molecular relaxation is thus obvious.

(ii) The equilibrium moisture uptake  $M_{\infty}$  is also relatively higher for samples which have more intense  $\tan \delta$  peaks with larger areas.

Next the role of the  $\alpha'$ -relaxation will be considered. The  $\alpha'$  peak is, broadly speaking, more intense for the 10 and 14.5 phr post-cured samples, which also have higher free volume and show much higher sorption rates at room temperature, compared to the corresponding standard-cure samples.

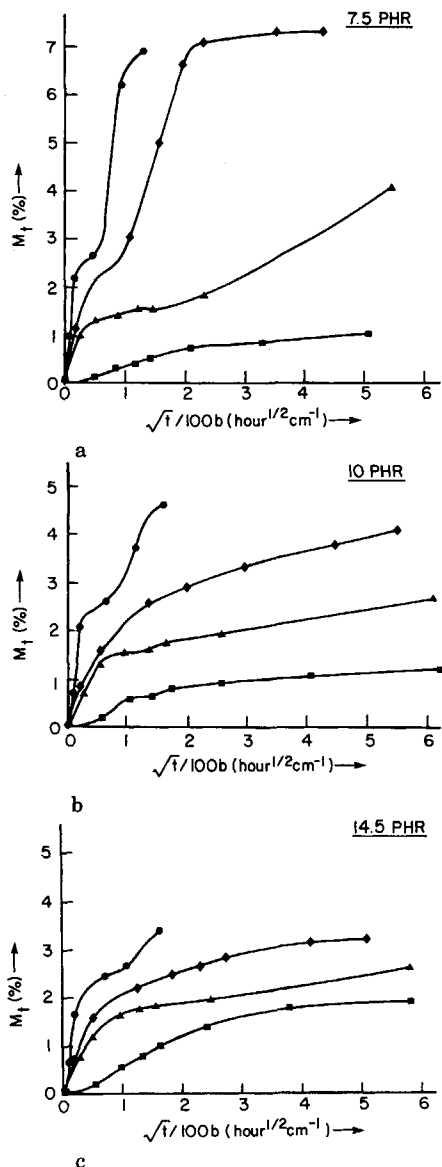


Fig. 20. Moisture sorption data for (a) 7.5, (b) 10, (c) 14.5, (d) 20, and (e) 25 phr standard-cure samples: (■) 20°C; (▲) 50°C; (◆) 75°C; (●) 100°C.

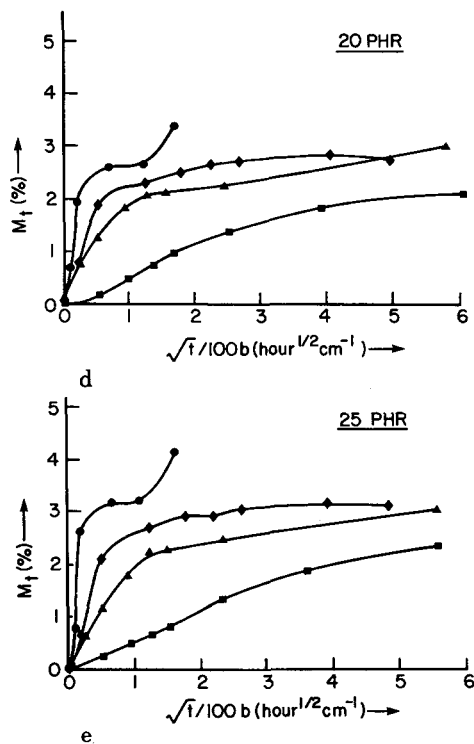


Fig. 20. (continued from previous page)

These observations suggest a qualitative correlation between moisture sorption and the relaxation process and provide a physical basis for the moisture transport characteristics of the various samples.

### Desorption Characteristics

The desorption characteristics of the postcured samples at 20 and 100°C are shown in Figure 24. For comparison the corresponding sorption data are also included. At room temperature desorption closely follows sorption, except perhaps for the 7.5 phr sample, while at 100°C the desorption is much more rapid. At intermediate temperatures the behavior is closer to 100°C, viz., the desorption process is in general faster than at 20°C. In Figure 24, the sorption and desorption envelopes have also been drawn at  $\sqrt{t}/b = 100$  (corresponding to a time of ca. 3 days) for the room temperature data and at  $\sqrt{t}/b = 15$  (corresponding to a time of ca. 2 h) for the 100°C data. As far as sorption is concerned, the features are similar to those already reported; viz., at room temperature, the high  $T_g$  samples (10 and 14.5 phr) which have high free volume, absorb more moisture. At 100°C these samples have low free volume and absorb less moisture. The desorption characteristics are, however, different. At room temperature, but for the 7.5 phr sample, the free volume dependence still exists; samples with high  $T_g$  and high free volume desorb the fastest. It was suggested earlier that the sorption at room temperature is predominantly a Langmuir, void-filling process.

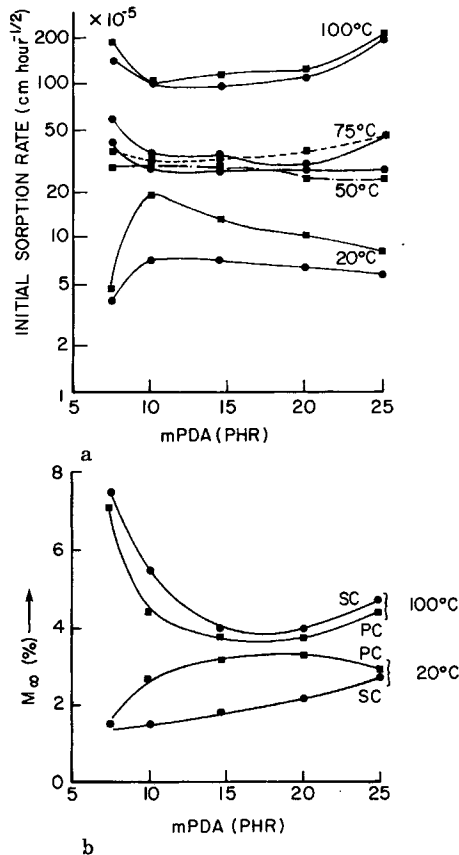


Fig. 21. (a) Initial sorption rate and (b) equilibrium moisture uptake for the standard-cure and postcured samples: (■) PC; (●) SC.

It would now appear that desorption is also similar in nature; the moisture leaves the voids as the sample desorbs. At 100°C, on the other hand, the desorption envelopes show two main differences: First, there is a significant time lag between sorption and desorption, and second, the free volume dependence is no longer present; in fact, the samples with the lowest free volume desorb the fastest. To explain these features, the physical bonds which are present in cured epoxy resin must be considered along with the effects of moisture on these bonds. The roles played by the hydroxyl and unreacted amine and epoxy groups in forming hydrogen bonds have been reported<sup>6,39</sup> in the literature, and the effect of moisture on these bonds has also been studied.<sup>40</sup> In the dry sample, the hydrogen bonds are strong, and sorption at 100°C must involve, in part, the breaking of some of these bonds. The water molecules which enter the sample attach themselves to these hydrogen-bond-forming groups either directly or indirectly through the water molecule. The bonds in the swollen polymer are relatively weak, and desorption is therefore faster. The second feature, viz. that the sample with the lowest free volume desorbs the fastest, also suggests that the strength of the bonds may be an important factor in determining desorption. The

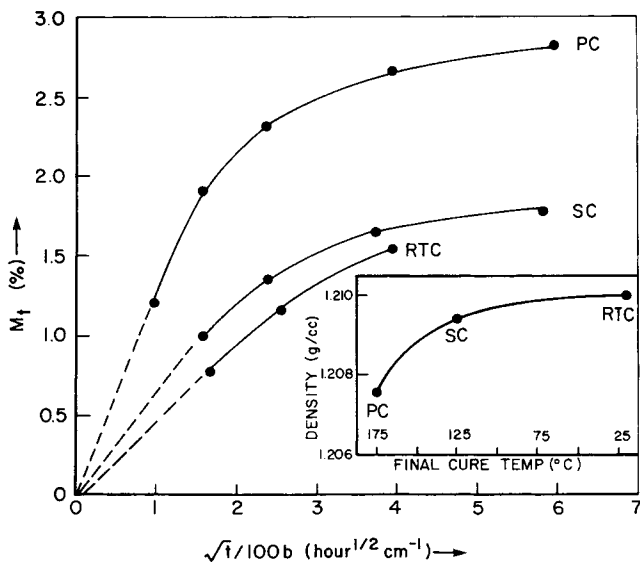


Fig. 22. Room-temperature sorption curves for stoichiometric samples with three cure cycles (inset: density data). RTC stands for room-temperature-cured.

stoichiometric sample has a relatively greater number of hydroxyl groups but very few unreacted amine and epoxy groups. The epoxy-rich samples contain hydroxyl groups and unreacted epoxy groups. The amine-rich samples contain hydroxyl groups and unreacted amine groups. Though an estimate of the number of hydrogen-bond-forming groups has not been made, it is likely that, as one moves away from stoichiometry on either side, the strength of the bonds between these groups and moisture increases and the desorption is therefore slower.

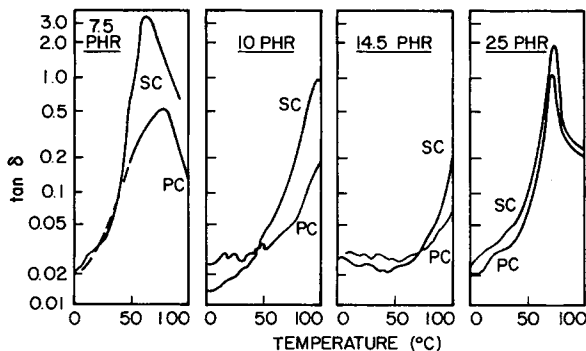


Fig. 23. The RMS  $\tan \delta$  curves for the dry standard-cure and postcured samples suitably shifted on the temperature axis to match their wet  $T_g$  (for details see text).

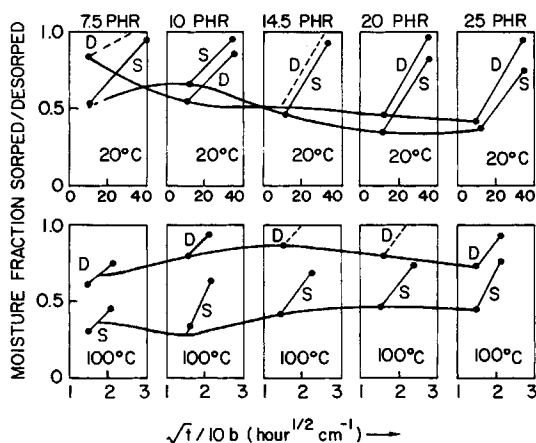


Fig. 24. Desorption data at 20 and 100°C (for comparison the corresponding sorption data are also included).

### The Role of Heterogeneous Morphology

The role of heterogeneous morphology could be important in two ways. First, the second stage of the sorption process observed distinctly in a number of samples could arise from moisture transport into the more densely crosslinked heterogeneities. It is observed that, as the temperature of sorption increases, the transition from the first to the second stage moves to shorter times. This could arise from relaxation processes which will make the more densely crosslinked regions accessible to moisture after the other regions are saturated. An alternative explanation attributes the second stage of moisture sorption to damage during moisture exposure, resulting in the formation of cavities which can absorb more moisture.<sup>1,4,41,42</sup> It has been postulated that such damage should not affect the sample  $T_g$ .<sup>43</sup> The glass transition temperatures of some post-cured stoichiometric samples which were exposed to a saturated moisture environment at 100°C for varying times were measured on the DSC. The DSC data of wet samples showed a splitting of  $T_g$ . In the 14.5 and 25 phr samples, the lower  $T_g$  was much more distinct. In the 7.5 phr sample, while the initial moisture sorption (1.17% after 20 min) resulted in two distinct  $T_g$ 's, it was observed that, in samples exposed to longer times, the upper  $T_g$  was much more prominent. The principal features of the results are shown in Figure 25 and suggest that moisture sorption at 100°C for long times might have resulted in some damage in the case of the 7.5 phr sample.

The samples of different stoichiometry exposed to moisture at 100°C were examined on an optical microscope. The 7.5 phr sample showed some signs of damage. To enhance the damage, a set of samples was prepared by exposing them to 100% relative humidity at 125°C. It was found that the 7.5 phr sample, which absorbed maximum moisture, also showed considerable damage. A typical micrograph (Fig. 26) shows the extensive damage. However, the other samples did not reveal much damage at that level. Studies on damage at a finer level have, however, not been made on these



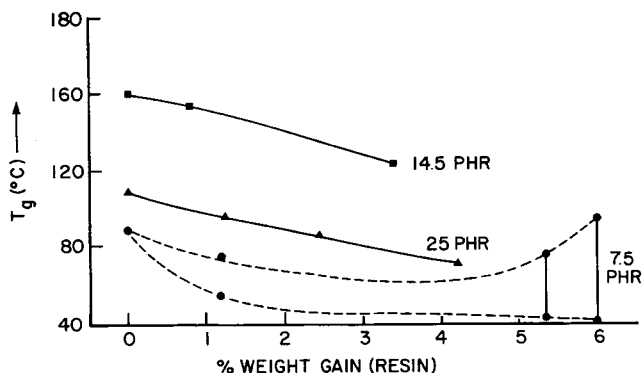


Fig. 25. The dependence of glass transition temperature on moisture content.

samples. It may thus be stated that while in some samples damage could play an important role in enhancing moisture sorption, in others heterogeneous morphology cannot be ruled out as a factor.

The second possible role played by the heterogeneities is their effect on the creation of voids with changing temperature. Since the expansion coefficients of the heterogeneities and the matrix will be expected to be different, biaxial stresses can develop in the matrix which, at lower temperatures, can result in dilatation of the matrix and creation of voids into which moisture can enter.

### CONCLUSIONS

The free volume at room temperature is apparently in the form of frozen voids, and moisture sorption/desorption at this temperature is of the Langmuir type with little or no bond formation. The free volume dependence of initial sorption rate at room temperature is very high and has been attributed to the distribution of free volume, which results in large mobility

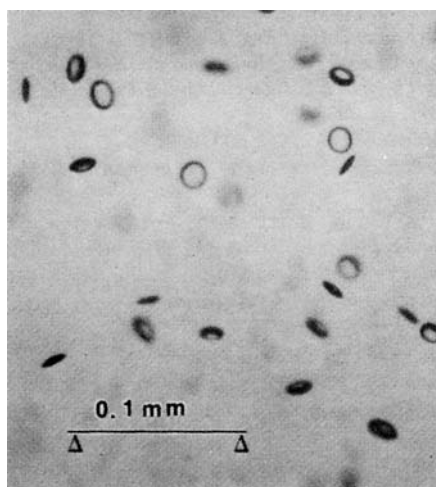


Fig. 26. Optical micrograph of 7.5 phr post-cured sample containing 5% moisture.

changes for relatively small variations in free volume. Apparently the  $\alpha'$  transition, which is a broad, weak transition close to room temperature, reflects this mobility and is moisture-sensitive. At higher temperatures the free volume is generated predominantly from segmental motion due to the onset of  $\alpha$  transition. The Henry's law mode becomes operative, and the moisture can now form bonds with suitable groups in the resin.

Two possible roles of heterogeneous morphology have been highlighted. First, the second stage of the sorption process observed distinctly in a number of samples could arise from moisture transport into the more densely crosslinked heterogeneities. The second possible role played by the heterogeneities is their effect on the creation of voids with changing temperature. This can result in higher free volume at lower temperatures.

The authors are grateful to R. Turner, J. Miller, H. Chin, and A. Biermann of UDRI for technical assistance and to Dr. C. Y.-C. Lee for helpful discussions. The assistance of the Sentry Co., Foxboro, MA, in encapsulating the samples is also gratefully acknowledged. One of the authors (V. B. Gupta) is grateful to the Air Force Systems Command and to the National Research Council, Washington, DC, for the award of an Associateship during 1982-84 and to the Indian Institute of Technology, New Delhi, India for the grant of leave.

### References

1. J. M. Whitney and C. E. Browning, in *Advanced Composite Materials — Environmental Effects*, ASTM Special Technical Publication 658, J. R. Vinson, Ed., Am. Soc. for Testing and Mater., Philadelphia, 1978, p. 43.
2. M. J. Adamson, *J. Mater. Sci.*, **15**, 1736 (1980).
3. Y. Diamant, G. Marom, and L. J. Broutman, *J. Appl. Polym. Sci.*, **26**, 3015 (1981).
4. A. Apicella, L. Nicolais, G. Astarita, and E. Drioli, *Polym. Eng. Sci.*, **21**, 18 (1981).
5. J. B. Enns and J. K. Gillham, *J. Appl. Polym. Sci.*, **28**, 2831 (1983).
6. J. L. Illinger and N. S. Schneider, *Polym. Eng. Sci.*, **20**, 310 (1980).
7. W. J. Mikols, J. C. Seferis, A. Apicella, and L. Nicolais, *Polym. Compos.*, **3**, 118 (1982).
8. P. Yang, L. Carlsson, and S. S. Sternstein, *Polym. Compos.*, **4**, 104 (1983).
9. J. D. Keenan, J. C. Seferis, and J. T. Quinlivan, *J. Appl. Polym. Sci.*, **24**, 2375 (1979).
10. A. Apicella, L. Nicolais, and J. C. Halpin, 28th National SAMPE Symposium, Vol. 28, 1983, p. 519.
11. D. Cohn and G. Marom, *Polymer*, **24**, 223 (1983).
12. P. Moy and F. E. Karasz, *Polym. Eng. Sci.*, **20**, 315 (1980).
13. J. Mijovic, *Ind. Eng. Chem., Prod. Res. Dev.*, **21**, 290 (1982).
14. R. Bruce Prime, in *Thermal Characterization of Polymeric Materials*, Edith A. Turi, Ed., Academic, New York, 1981, p. 435.
15. L. E. Nielsen, *J. Macromol. Sci.*, **C3**, 69 (1969).
16. L. E. Nielsen, *Mechanical Properties of Polymers and Composites*, Dekker, New York, 1974, Vol. I.
17. S. Sourour and M. R. Kamal, *Thermochim. Acta*, **14**, 41 (1976).
18. M. G. Elias, *Macromolecules 1: Structure and Properties*, Plenum, New York, 1978, p. 378.
19. J. D. Ferry, *Viscoelastic Properties of Polymers*, 2nd ed., Wiley, New York, 1970.
20. Y. S. Lipatov, in *Advances in Polymer Science 26: Conformation and Morphology*, Springer-Verlag, Heidelberg, 1978.
21. S. Matsuoka, *Polym. Eng. Sci.*, **21**, 907 (1981).
22. R. N. Haward, *Physics of Glassy Polymers*, Halstead, New York, 1976, pp. 27-39.
23. L. C. E. Struik, *Physical Aging in Amorphous Polymers and Other Materials*, Elsevier, New York, 1978.
24. Frank Weaver, "Epoxy Adhesive Surface Energies via the Pendant Drop Method," Air Force Technical Report, AFWAL-TR-82-4179, AFWAL Materials Laboratory, Wright-Patterson AFB, OH 45433.
25. T. D. Chang, S. H. Carr, and J. O. Brittain, *Polym. Eng. Sci.*, **22**, 1219 (1982).

26. V. B. Gupta, L. T. Drzal, C. Y-C. Lee, and M. J. Rich, *J. Macromol. Sci. Phys.* to appear.
27. R. Deiasi and J. B. Whiteside, in *Advanced Composite Materials — Environmental Effects*, ASTM Special Technical Publication 658, J. R. Vinson, Ed., Am. Soc. for Testing and Mater., Philadelphia, 1978, p. 12.
28. V. B. Gupta, L. T. Drzal, C. Y-C. Lee, and M. J. Rich, *Am. Chem. Soc. Polym. Prepr.*, **24**, 5 (1983).
29. V. B. Gupta, L. T. Drzal, W. W. Adams, and R. Omlor, *J. Mater. Sci.*, to appear.
30. H. H. Cohen and D. Turnbull, *J. Chem. Phys.*, **31**, 1164 (1959).
31. V. T. Stannet, W. S. Koros, D. R. Paul, H. K. Lonsdale, and R. W. Baker, in *Advances in Polymer Science*, N. J. Cantow et al., Eds., Springer-Verlag, Berlin, 1979.
32. A. Michaels, W. R. Vieth, and J. A. Barrie, *J. Appl. Polym. Sci.*, **34**, 1 (1963).
33. T. G. Fox and P. J. Flory, *J. Appl. Phys.*, **21**, 581 (1951).
34. M. L. Williams, R. F. Landel, and J. D. Ferry, *J. Am. Chem. Soc.*, **77**, 4701 (1955).
35. C. J. Patton, R. M. Felder, and W. J. Koros, *J. Appl. Polym. Sci.*, **29**, 1095 (1984).
36. D. T. Turner, *Polymer*, **23**, 197 (1982).
37. E. E. Labarre and D. T. Turner, *J. Polym. Sci., Polym. Phys. Ed.*, **20**, 557 (1982).
38. G. Kraus and J. T. Gruver, *J. Appl. Polym. Sci., A-2*, **8**, 571 (1970).
39. F. Cangelosi and M. T. Shaw, *Polym. Plast. Technol. Eng.*, **21**(1), 13 (1983).
40. M. K. Antoon, J. L. Koenig, and T. Serafini, *J. Polym. Sci., Polym. Phys. Ed.*, **19**, 1569 (1981).
41. R. J. Morgan and J. E. O'Neal, *Polymer Plast. Tech. Eng.*, **10**, 49 (1978).
42. R. J. Morgan, J. E. O'Neal, and D. L. Fanter, *J. Mater. Sci.*, **15**, 751 (1980).
43. C. E. Browning, G. E. Husman, and J. M. Whitney, in *Composite Materials; Testing and Design (Fourth Conference)*, ASTM Special Technical Publication 617, Am. Soc. for Testing and Mater., Philadelphia, 1977, p. 481.

Received July 3, 1984

Accepted February 28, 1985